

NJC

Accepted Manuscript



This is an *Accepted Manuscript*, which has been through the Royal Society of Chemistry peer review process and has been accepted for publication.

Accepted Manuscripts are published online shortly after acceptance, before technical editing, formatting and proof reading. Using this free service, authors can make their results available to the community, in citable form, before we publish the edited article. We will replace this *Accepted Manuscript* with the edited and formatted *Advance Article* as soon as it is available.

You can find more information about *Accepted Manuscripts* in the [Information for Authors](#).

Please note that technical editing may introduce minor changes to the text and/or graphics, which may alter content. The journal's standard [Terms & Conditions](#) and the [Ethical guidelines](#) still apply. In no event shall the Royal Society of Chemistry be held responsible for any errors or omissions in this *Accepted Manuscript* or any consequences arising from the use of any information it contains.

Cite this: DOI: 10.1039/c0xx00000x

www.rsc.org/xxxxxx

ARTICLE TYPE

Synthesis and Characterization of Cd₄YbO(BO₃)₃ – A Congruent Melting Cadmium-oxyborates with Large Nonlinear Optical Properties

Guohong Zou,*^a Ling Huang,^a Huaqiang Cai,*^a Shichao Wang,^b and Ning Ye*^b

Received (in XXX, XXX) Xth XXXXXXXXXX 20XX, Accepted Xth XXXXXXXXXX 20XX

DOI: 10.1039/b000000x

A nonlinear optical crystal cadmium-ytterbium oxyborates Cd₄YbO(BO₃)₃ has been synthesized through high-temperature solid-state reactions. In the crystal structure, CdO_n (n = 6, 8), YbO₆ distorted polyhedra and π -delocalization BO₃ groups interconnect via shared edges and corners to form a complicated three-dimensional (3D) network. The second harmonic generation (SHG) measurement shows that Cd₄YbO(BO₃)₃ possesses a large SHG response about four times as that of KH₂PO₄ (KDP) and is phase-matchable in the visible region. In addition, it exhibits a wide transparent regions ranging from near UV to middle IR. The title compound melts congruently suggesting that this material is a promising NLO material.

Introduction

Nonlinear-optical (NLO) materials,¹ as frequency conversion devices for providing coherent radiation in a wide-wavelength range, play an indispensable role in laser science and technology. Thus, they have attracted much attention. However it is particularly difficult to search for suitable materials with high NLO coefficients and wide transparency. It presents a great challenge to design new crystal materials with a preset function by an inorganic crystal engineering method. Employing noncentrosymmetric (NCS)² chromophores as building units offers a great strategy for synthesizing new NLO materials. Noncentrosymmetric (NCS) building units consist of distorted polyhedra with a d⁰ cation center resulting from a second-order Jahn–Teller effect,³ polar displacement of a d¹⁰ cation center,⁴ or distortion from the stereochemically active lone pair (SCALP) effect of the cation,⁵ or borate π -orbital systems.⁶ It has been demonstrated that the combination of the above two types of polarization groups can produce compounds with excellent SHG properties such as Pb₂B₅O₉I,⁷ BaMo₂TeO₉,^{3a} BaNbO(IO₃)₆.⁸

In the past decades, borates⁹ with π -conjugated systems have been widely considered as an ideal candidate for designing new NLO materials because of their wide transparency, noncentrosymmetric (NCS) structure types, high damage threshold, and high optical quality. In order to further enhance the second harmonic generation (SHG), Chen's group^{4a} employed the d¹⁰ cation Cd²⁺ with polar displacement and the Bi³⁺ cation with SCALP effect to be incorporated in borates, resulting in the discovery of a new NLO material Cd₄BiO(BO₃)₃ with strong SHG responses which is 6 times as that of KDP. However, it is known that introducing the BiO₆ distorted octahedron into borates may make the UV absorption edge shift sharply towards the red. In the present research, we introduced rare earth (Re) to substitute

for bismuth in the Bi₂O₃-CdO-B₂O₃ system because the NLO materials containing rare earth elements are with shorter UV absorption edge and excellent physicochemical properties such as YAl₃(BO₃)₄ (YAB),¹⁰ Y_{0.57}La_{0.72}Sc_{2.71}(BO₃)₄ (YLSB)¹¹ and GdCa₄(BO₃)₃ (GCOB).¹² Guided by this idea, our exploration of the CdO-B₂O₃-Re₂O₃ (Re = La, Sc, Yb) system leads to the discovery of a new UV NLO material, Cd₄YbO(BO₃)₃ with a wide transparent regions ranging from UV to middle IR and a large SHG effect, measured on ground crystals, about four times that of KDP. Herein we report the syntheses, crystal structures, and optical properties.

Experimental Section

Reagents

CdCO₃ (99%), H₃BO₃ (99%) and Yb₂O₃ (99.99%) were purchased from Sinopharm and used as received.

Synthesis

Single crystals of Cd₄YbO(BO₃)₃ was grown through high-temperature solid state reactions. A mixture of CdCO₃ (8.0 mmol), H₃BO₃ (6.0 mmol) and Yb₂O₃ (1.0 mmol) in a molar ratio of 8 : 6 : 1 were ground and loaded into platinum crucibles. The synthesis was performed in four steps. First, the mixtures were heated at 500 °C for one day in order to decompose H₃BO₃ and CdCO₃. Second, the resulting mixtures were further heated for one day at 1200 °C until transparent and clear melts were formed. Third, the melts were allowed to cool slowly (3 °C/h) to the final crystallization temperature (1100 °C). Finally, the obtained mixtures were quenched to room temperature. Colorless, transparent crystals were obtained for structure determination. After proper structural analysis, pure powder samples of Cd₄YbO(BO₃)₃ were obtained in quantitative yield through the

Table 1. Crystal Data and Structure Refinement for $\text{Cd}_4\text{YbO}(\text{BO}_3)_3$.

Formula	$\text{Cd}_4\text{YbO}(\text{BO}_3)_3$
Formula Mass (amu)	815.07
Crystal System	Monoclinic
Space Group	<i>Cm</i>
a (Å)	7.938 (4)
b (Å)	15.794 (7)
c (Å)	3.4414(15)
β (°)	99.992(9)
V(Å ³)	424.9(3)
Z	2
ρ (calcd) (g/cm ³)	6.370
Temperature (K)	293(2)
λ (Å)	0.71073
F(000)	714
μ (mm ⁻¹)	20.79
Final R indices ($I > 2\sigma(I)$) ^a R_1/wR_2	0.0527/0.1367
R indices (all data) ^a R_1/wR_2	0.0545/0.1380
GOF on F^2	1.11
Absolute Structure Parameter	0.00

$$^a R_1(F) = \frac{\sum ||F_o| - |F_c||}{\sum |F_o|}, wR_2(F_o^2) = \frac{[\sum w(F_o^2 - F_c^2)^2 / \sum w(F_o^2)^2]}{1/2}$$

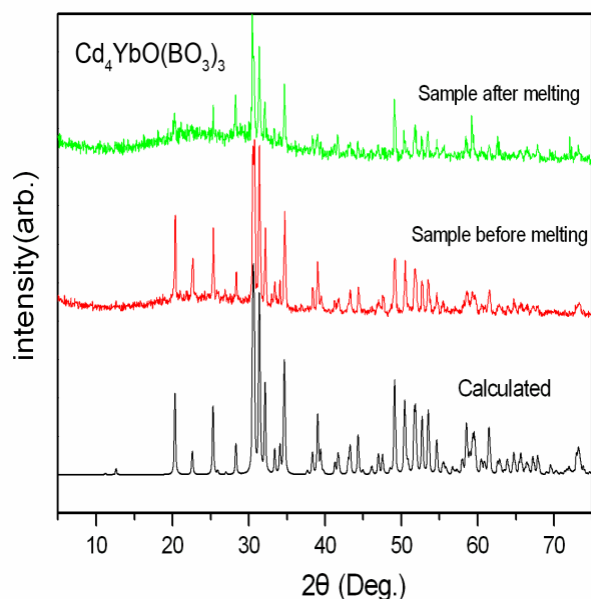


Figure 1: Experimental and calculated XRD patterns for $\text{Cd}_4\text{YbO}(\text{BO}_3)_3$. The black curve is the calculated one, the red is the pattern of sample before melting and the green is the pattern of sample after melting.

Table 2. Atomic coordinates and equivalent isotropic displacement parameters for $\text{Cd}_4\text{YbO}(\text{BO}_3)_3$. U_{eq} is defined as one third of the trace of the orthogonalized U_{ij} tensor.

atom	x	y	z	$U_{eq}(\text{Å}^2)$	BVS
Yb(1)	0.0227(2)	0.5000	0.6932(3)	0.015(1)	2.615
Cd(1)	0.3790(2)	0.3879(1)	0.3596(3)	0.002(1)	2.068
Cd(2)	0.2642(1)	0.1738(1)	0.0552(5)	0.009(1)	1.717
O(1)	0.1990(30)	0.5000	0.2750(40)	0.008(3)	1.809
O(2)	0.5490(30)	0.2719(13)	0.3900(50)	0.021(2)	1.876
O(3)	0.2370(30)	0.3213(11)	0.8070(60)	0.010(2)	1.936
O(4)	0.0670(20)	0.0768(11)	-0.0590(40)	0.012(3)	2.123
O(5)	0.4360(20)	0.1414(12)	-0.3880(40)	0.016(3)	1.944
O(6)	-0.1700(18)	0.5000	1.1070(90)	0.029(3)	1.700
B(1)	0.1400(20)	0	-0.0190(50)	0.004(6)	2.884
B(2)	0.0770(30)	0.3005(17)	0.6110(70)	0.006(4)	2.815

¹⁰ solid-state reactions from the stoichiometric mixtures of CdCO_3 , H_3BO_3 and Yb_2O_3 at 950 °C for 5 days.

Single Crystal X-ray Diffraction

Single crystal X-ray diffraction data were collected at room temperature on a Rigaku Mercury CCD diffractometer with graphite-monochromatic Mo K α radiation ($\lambda = 0.71073$ Å). A transparent block of crystal was mounted on a glass fiber with epoxy for structure determination. A hemisphere of data was collected using a narrow-frame method with the ω -scan mode. The data were integrated using the CrystalClear program, and the intensities were corrected for Lorentz polarization, air absorption, and absorption attributable to the variation in the path length through the detector faceplate. Absorption corrections based on the Multiscan technique¹³ were also applied. The structure was solved by the direct methods and refined by full-matrix least-squares fitting on F^2 using SHELX-97.¹⁴ All of the structures were verified using the ADDSYM algorithm from the program PLATON,¹⁵ and no higher symmetries were found. Relevant crystallographic data and details of the experimental conditions for $\text{Cd}_4\text{YbO}(\text{BO}_3)_3$ are summarized in Table 1. Atomic coordinates and isotropic displacement coefficients are listed in Table 2. Selected bond lengths and angles (deg) for $\text{Cd}_4\text{YbO}(\text{BO}_3)_3$ are listed in Table 3.

Powder X-ray Diffraction

X-ray diffraction patterns of polycrystalline materials were obtained on a Rigaku Dmax2500 powder X-ray diffractometer by using Cu K α radiation ($\lambda = 1.540598$ Å) at room temperature in the angular range of $2\theta = 5$ -75° with a scan step width of 0.05° and a fixed time of 0.2 s. The powder XRD patterns for the pure

Table 3. Selected bond lengths (Å) and angles (deg) for Cd₄YbO(BO₃)₃.^a

Yb1—O1	2.17 (2)	Yb1—O6 ⁱⁱ	2.31 (3)
Yb1—O1 ⁱ	2.24 (2)	Yb1—O5 ⁱⁱⁱ	2.340 (19)
Yb1—O6	2.26 (3)	Yb1—O5 ^{iv}	2.340 (19)
Cd1—O1	2.263 (15)	B1—O4 ^{xiii}	1.34 (2)
Cd1—O2	2.27 (2)	B1—O6 ^x	1.49 (5)
Cd1—O3 ⁱⁱ	2.291 (19)	B2—O2 ^{viii}	1.37 (3)
Cd1—O3	2.310 (19)	B2—O5 ⁱⁱⁱ	1.45 (3)
Cd1—O4 ^{vi}	2.314 (15)	O4 ^{xiii} —B1—O4	129 (3)
Cd1—O4 ^{vii}	2.346 (15)	O4 ^{xiii} —B1—O6 ^x	115.3 (17)
Cd2—O5 ⁱ	2.226 (18)	O4—B1—O6 ^x	115.3 (17)
Cd2—O4	2.228 (18)	O2 ^{viii} —B2—O3	121 (2)
Cd2—O5	2.289 (17)	O2 ^{viii} —B2—O5 ⁱⁱ	119 (2)
Cd2—O2 ^{vii}	2.356 (19)	O3—B2—O5 ⁱⁱ	120 (2)
Cd2—O3 ⁱⁱ	2.413 (18)		

^a Note. Symmetry transformations used to generate equivalent atoms: (i) $x, y, z+1$; (ii) $x, y, z-1$; (iii) $x-1/2, -y+1/2, z+1$; (iv) $x-1/2, y+1/2, z+1$; (v) $x, -y+1, z$; (vi) $x+1/2, -y+1/2, z$; (vii) $x+1/2, -y+1/2, z+1$; (viii) $x-1/2, -y+1/2, z$; (ix) $x+1/2, y-1/2, z-1$; (x) $x+1/2, y-1/2, z$; (xi) $x-1/2, -y+1/2, z-1$; (xii) $x+1/2, -y+1/2, z-1$; (xiii) $x, -y, z$.

powder samples of Cd₄YbO(BO₃)₃ showed good agreement with the calculated XRD patterns from the single-crystal models (Figure 1).

10 Thermal Analysis

Differential thermal analysis (DTA) was performed under nitrogen atmosphere on a NETZSCH DTA404PC. The sample and reference (Al₂O₃) were enclosed in Pt crucibles, heated from room temperature to 1200 °C for Cd₄YbO(BO₃)₃ and then allowed to cool to 100 °C at a rate of 10 °C/min.

Infrared Spectroscopy

IR spectra were recorded on a Magna 750 Fourier transform infrared (FT-IR) spectrometer as KBr pellets in the range of 4000-400 cm⁻¹.

20 UV-vis Diffuse Reflectance Spectroscopy

The UV-vis diffuse reflection data were recorded at room

temperature using a powder sample with BaSO₄ as a standard (100% reflectance) on a PerkinElmer Lambda-900 UV/vis/NIR spectrophotometer and scanned at 200-2500 nm. Reflectance spectra were converted to absorbance using the Kubelka-Munk function.¹⁶

Second-Harmonic Generation

Powder second-harmonic generation (SHG) signals were measured using the experimental method adapted from that reported by Kurtz and Perry¹⁷ with the wavelength of the fundamental (1064 nm doubled to 532 nm). Since SHG efficiencies were known to be strongly dependent on particle size, polycrystalline samples were ground and sieved into the following particle size ranges: 20-44, 44-74, 74-105, 105-149, and 149-210 μm. In order to make relevant comparisons with known SHG materials, crystalline KDP were also ground and sieved into the same particle size ranges. The samples were pressed between glass microscope cover slides and secured with tape in 1-mm thick aluminum holders containing an 8-mm diameter hole. They were subsequently placed in a light-tight box and irradiated with a pulsed infrared beam (10 ns, 3 mJ, 10 Hz) from a Q-switched Nd: YAG laser at a wavelength of 1064 nm. A cutoff filter was used to limit background flash-lamp light on the sample, and an interference filter (530 ± 10 nm) was used to select the second harmonic for detection with a photomultiplier tube attached to a RIGOL DS1052E 50-MHz oscilloscope. This procedure was then repeated using the standard nonlinear optical material KDP, and the ratio of the second-harmonic intensity outputs was calculated. No index-matching fluid was used in any of the experiments.

Computational Descriptions.

First principle band structure and density of states (DOS) calculations were carried out by employing the plane-wave basis pseudopotential method as implemented in the CASTEP.¹⁸ The exchange and correlation effects were considered by Perdew–Burke–Ernzerhof (PBE) in the generalized gradient approximation (GGA).¹⁹ Norm-conserving pseudopotentials are selected to describe the interactions between the ionic cores and the valence electrons.²⁰ In the atoms, B: 2s²2p¹, O: 2s²2p⁴, Cd: 4d¹⁰5s², Yb: 4f¹⁴5s²5p⁶6s², were treated as valence electrons. A kinetic-energy cutoff of 700 eV was set for the self-consistent-field convergence of the total electronic energy. Monkhorst–Pack *k*-point meshes with a density of 4 × 4 × 7 points in the Brillouin zone of the Cd₄YbO(BO₃)₃ unit cell are chosen. The other parameters and convergence criteria were adopted the default values of the CASTEP code.

Results and Discussion

Crystal Structure

Cd₄YbO(BO₃)₃ is isostructural to its Bi derivative Cd₄BiO(BO₃)₃ and crystallize into a monoclinic crystal system with an acentric space group of *Cm*. Its structure is an intricate three-dimensional (3D) framework of interconnecting Cd1O₆, Cd2O₈ and Yb1O₆ distorted polyhedra, and π -delocalization BO₃ planar triangles as shown in Figures 2a and 2b. There are two kinds of boron sites, B(1) and B(2), with three-fold coordination. BO₃ planar triangles with B-O bond lengths ranging from 1.34 (2) to 1.49 (5) Å lie

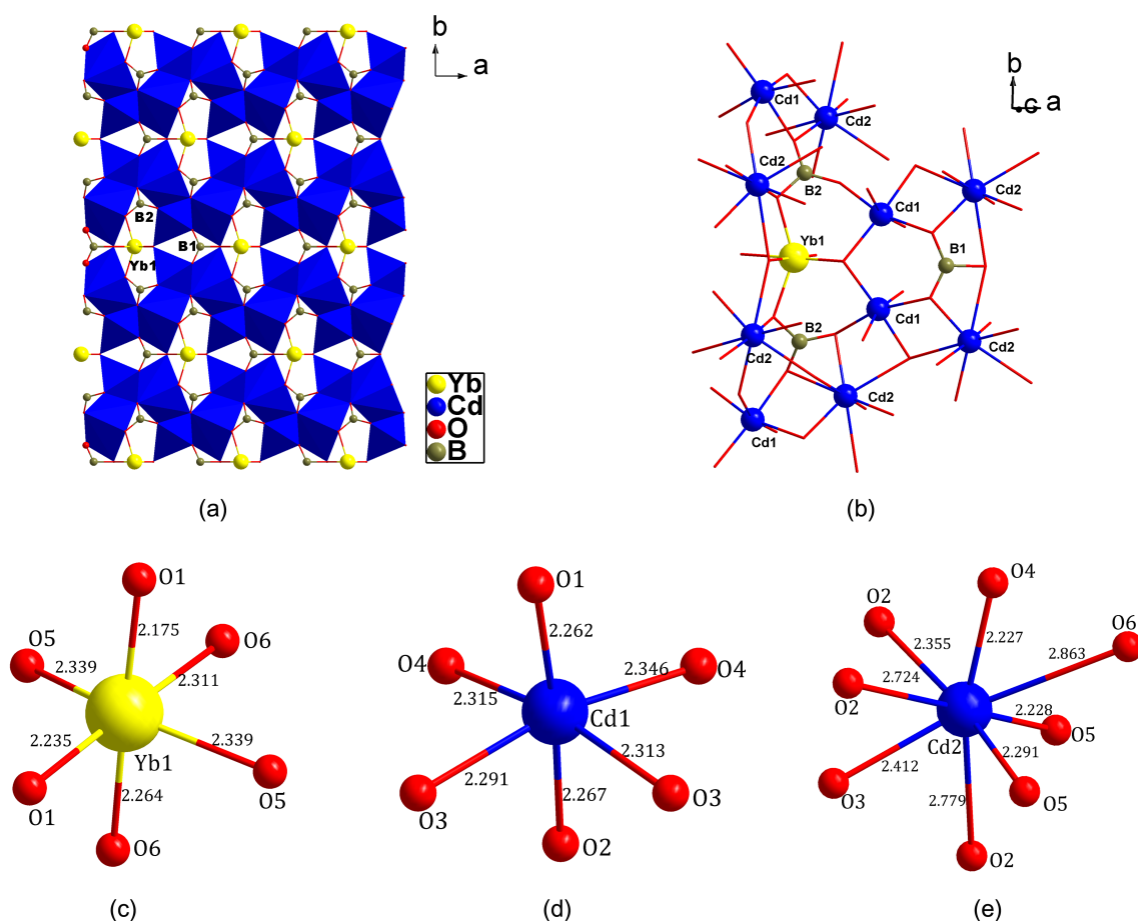


Figure 2: View of the structure of Cd₄YbO(BO₃)₃ down the c axis (a) and cation coordinate environments (b), and the coordination of oxygen atoms around Yb1 (c), Cd1 (d), and Cd2 (e) cations.

5 approximately parallel to the (001) plane. In this structure, all the BO₃ planar triangles are approximately parallel along the c axis that produces cooperative contribution to the macroscopic SHG effect. There are two types of Cd²⁺ ions that occupy distorted polyhedra sites: Cd1O₆, Cd2O₈ distorted polyhedra (Figure 2c).
 10 The Cd–O bond lengths range from 2.262 – 2.346 Å in Cd1O₆ distorted polyhedra, and 2.227 – 2.863 Å in Cd2O₈ distorted polyhedra. Each Cd1O₆ distorted octahedron shares corners with five BO₃ triangles, while every Cd2O₈ distorted dodecahedron shares corners with two and edges with three BO₃ triangles.
 15 Along the c axis, Cd1O₆ and Cd2O₈ distorted polyhedra interconnect via sharing edges and corners into 1D double chains. The double chains are further interconnected via sharing corners and edges into a 3D framework with the eight-member and four-member tunnels. Then, the B2 and Yb atoms are located in eight-member tunnels, while the B1 atoms are located in four-member tunnels. The Yb³⁺ cation is surrounded by six oxygen atoms, forming a YbO₆ distorted octahedron with Yb–O bond lengths ranging from 2.175 to 2.339 Å, and the octahedron shares corners with four BO₃ triangles.

25 The bond valence sums for Cd₄YbO(BO₃)₃ is calculated using

the formula

$$V_i = \sum S_{ij} = \sum \exp\left\{\left(r_0 - r_{ij}\right)/B\right\} \quad (1)$$

where S_{ij} is the bond valence associated with bond length r_{ij} and r_0 and B (usually 0.37) are empirically determined parameters.²¹

30 The calculated total bond valence for Cd, Yb, B, and O atoms are summarized in Table 2. These valence sums are in good agreement with the expected oxidation states which suggest that the reported crystal structure is correct.

Thermal Properties

35 The DSC diagrams of Cd₄YbO(BO₃)₃ exhibit one endothermic peak in the heating curves and one exothermic peaks in the cooling curves, revealing that it melts congruently at around 1150 °C (Figure 3). To verify that Cd₄YbO(BO₃)₃ melts congruently, Cd₄YbO(BO₃)₃ powders were placed into a platinum crucible and
 40 heated to 1200 °C until the powders melted completely. The powders were allowed to cool to room temperature. Analysis of the powder XRD patterns of the solidified melts reveals that the solid products exhibit a diffraction pattern identical to that of the initial compound powders (Figure 1), further demonstrating that

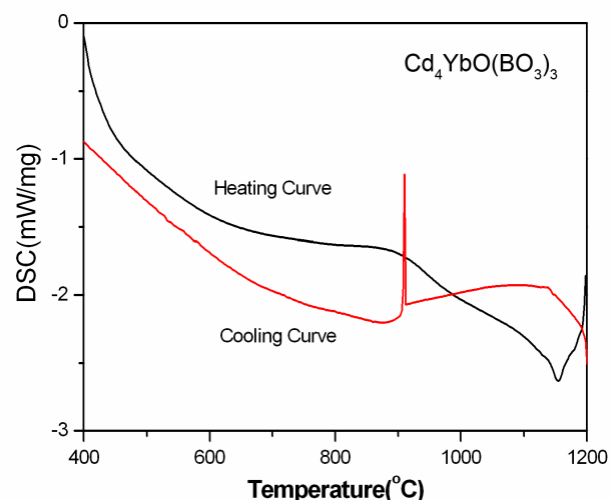


Figure 3: DSC curves of $\text{Cd}_4\text{YbO}(\text{BO}_3)_3$

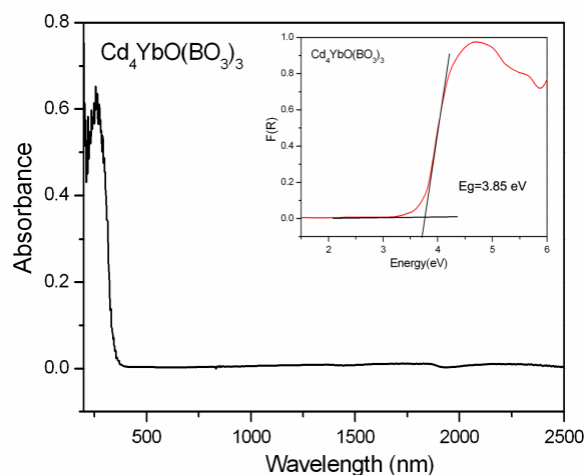


Figure 4: UV absorption spectra and Optical diffuse reflectance spectra of $\text{Cd}_4\text{YbO}(\text{BO}_3)_3$

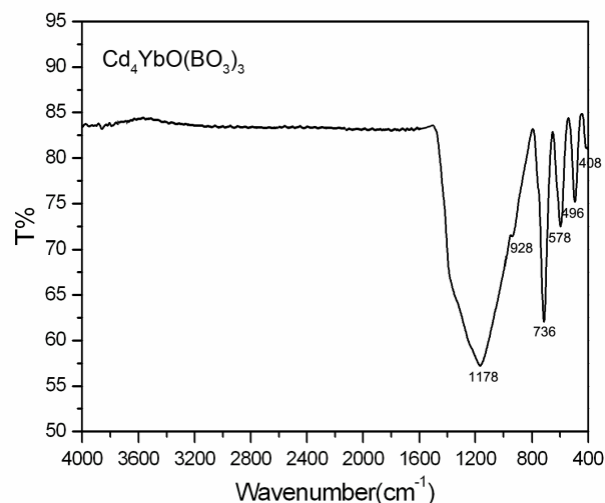


Figure 5: IR spectra for $\text{Cd}_4\text{YbO}(\text{BO}_3)_3$.

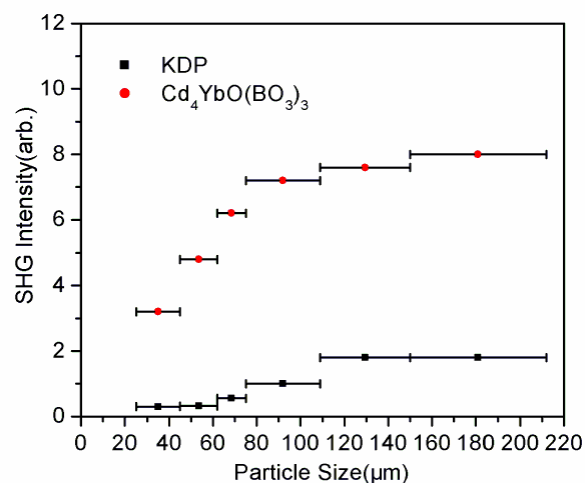


Figure 6: SHG measurements of $\text{Cd}_4\text{YbO}(\text{BO}_3)_3$ ground crystals (solid circle) with KDP (open circle) as a reference (1064 nm doubled to 532 nm).

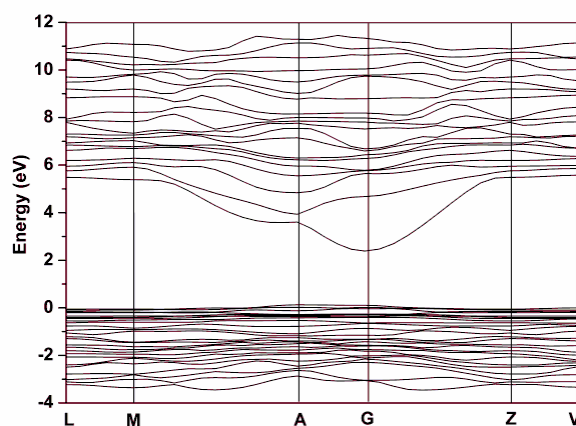


Figure 7: Band structure for $\text{Cd}_4\text{YbO}(\text{BO}_3)_3$.

$\text{Cd}_4\text{YbO}(\text{BO}_3)_3$ is congruent melting compounds. This behavior indicates that its single crystals with large size and high quality could be grown by the Czochralski method.

Optical Properties

UV-Vis diffuse reflectance spectra was collected for $\text{Cd}_4\text{YbO}(\text{BO}_3)_3$. Absorption (K/S) data were calculated from the following Kubelka-Munk function: $F(R) = (1-R)^2/2R = K/S$, where R is the reflectance, K is the absorption, and S is the scattering. In the (K/S)-versus- E plots, extrapolating the linear part of the rising curve to zero provides the onset of absorption. UV absorption spectra of $\text{Cd}_4\text{YbO}(\text{BO}_3)_3$ reveals that it has wide transparent regions ranging from near UV to middle IR (Figure 4). Optical diffuse reflectance spectrum studies indicate that the optical band gap for $\text{Cd}_4\text{YbO}(\text{BO}_3)_3$ are approximately 3.85 eV with UV cut-off edge of 322 nm (Figure 4). Compared with its isostructural compound $\text{Cd}_4\text{BiO}(\text{BO}_3)_3$ whose UV cut-off edge is about 392 nm, $\text{Cd}_4\text{YbO}(\text{BO}_3)_3$ has a shorter UV cut-off edge that demonstrates the introduction of rare earth to substitute for bismuth can effectively produce the blue shift of the UV absorption edge.

Figure 5 presents the IR spectra of $\text{Cd}_4\text{YbO}(\text{BO}_3)_3$. Referring

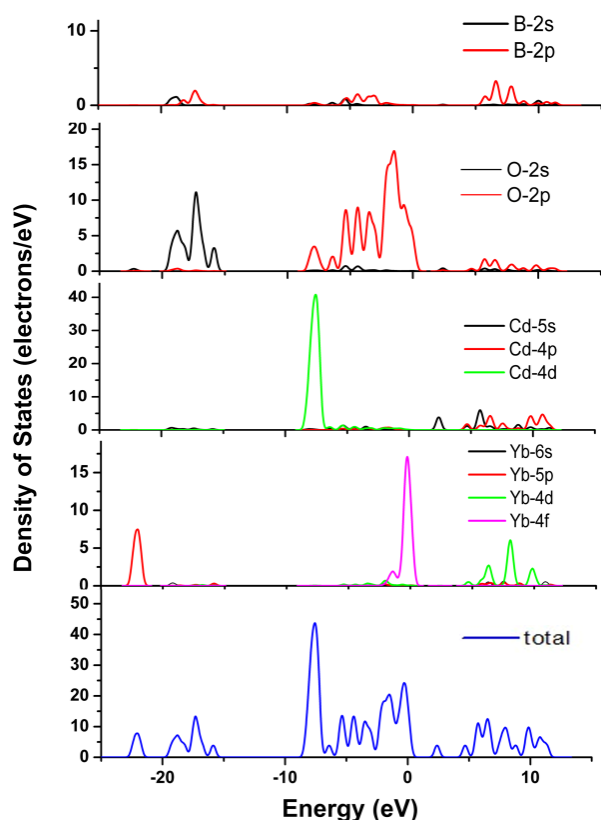


Figure 8: Total and partial densities of states for $\text{Cd}_4\text{YbO}(\text{BO}_3)_3$.

to the literature,²² the peaks at 1178 and 928 cm^{-1} for $\text{Cd}_4\text{YbO}(\text{BO}_3)_3$ can be assigned to asymmetric stretching and symmetric stretching vibrations of BO_3 , while the peaks located at 736 cm^{-1} is likely from the out-of-plane bending of B–O in BO_3 . The peaks at 578, 496 and 408 cm^{-1} are attributed to bending vibrations.

NLO Properties

The curves of SHG signal as a function of particle size from the measurements made on ground crystals for $\text{Cd}_4\text{YbO}(\text{BO}_3)_3$ are shown in Figure 6. The results are consistent with phase-matching behaviors according to the rule proposed by Kurtz and Perry.¹⁷ A KDP sample is selected as a reference. The second-harmonic signal is found to be $4 \times$ KDP for $\text{Cd}_4\text{YbO}(\text{BO}_3)_3$. Since the reported d_{36} coefficient for KDP is 0.39 pm/V ,²³ the derived d_{eff} coefficients for $\text{Cd}_4\text{YbO}(\text{BO}_3)_3$ is 1.56 pm/V . In the $\text{Cd}_4\text{BiO}(\text{BO}_3)_3$,^{4a} the main sources of the SHG response are from the cooperation of the 3-chromophore asymmetric structures composed of the polar displacement of the d^{10} Cd^{2+} ion, SCALP effect of Bi^{3+} , and π -delocalization of BO_3 . So we believe that the cooperation effects of the asymmetric π -delocalization of the triangular BO_3 groups and the polar displacement of the d^{10} cation Cd^{2+} and YbO_6 distorted octahedron in $\text{Cd}_4\text{YbO}(\text{BO}_3)_3$ make the material exhibit a large SHG response.

Calculations

To gain further insight the bonding interactions in $\text{Cd}_4\text{YbO}(\text{BO}_3)_3$,

theoretical calculations were performed based on DFT methods. As plotted in Figure 7, the calculated band structure along high-symmetry points of the first Brillouin zone information was presented. It is clear that both the conduction band minimum and the valence band maximum are localized at the G point, with a direct band gap of 2.28 eV. The total and partial densities of states, DOS and PDOS are presented in Figure 8. The occupied part of the valence band can be subdivided into four regions separated by energy gaps. The bands in the lowest region, from -51.0 eV to -49.0 eV, have most of the contribution from the s orbital of Yb. The valence bands (VB) spanning over -23.0 eV to -21.0 eV originate predominately from Yb-5p, while from -20 eV to -15.0 eV have the most of the contributions from O-2s, B-2s and B-2p states. In the vicinity of the Fermi level, namely, from -9.0 eV to 0 eV in the valence band, Cd-4d, O-2p, Yb-4d4f, and B-2p states are mainly involved and overlap fully, indicative of the strong covalent interactions of Cd–O, Yb–O, B–O bonds. Energy band around 2.5 eV regions is made up of the Cd-5s state. Ranging from 4.3 eV to 11.0 eV in the conduction band, the Yb-5d, O-2p, B-2p, and Cd-4p5s states are mainly involved.

Conclusions

In summary, we discovered a novel ultraviolet nonlinear-optical material $\text{Cd}_4\text{YbO}(\text{BO}_3)_3$ in the $\text{CdO}-\text{Yb}_2\text{O}_3-\text{B}_2\text{O}_3$ system. In the crystal structure, Cd_4O_6 , Cd_2O_8 and YbO_6 distorted polyhedra interconnect via shared edges and corners into a three dimensional framework with tunnels along the c axis, where all B atoms are located. Isolated BO_3 planar triangles lie approximately parallel to the (001) plane in the space of the framework. The second harmonic generation test shows that the compound exhibits a large second harmonic generation response about four times that of KH_2PO_4 . Moreover, the ultraviolet – visible – infrared diffuse reflectance spectrum indicates that $\text{Cd}_4\text{YbO}(\text{BO}_3)_3$ has a wide transparent region from the ultraviolet to near infrared regions. It is congruent melting compounds with excellent physicochemical properties. These features promise $\text{Cd}_4\text{YbO}(\text{BO}_3)_3$ great applications as a nonlinear-optical material.

Acknowledgments

This research was supported by the National Natural Science Foundation of China (Nos. 91222204 and 21401178), Main Direction Program of Knowledge Innovation of Chinese Academy of Sciences (Grant No. KJCX2-EW-H03-03), Special Project of National Major Scientific Equipment Development of China (No. 2012YQ120060) and Science and Technology Innovation Foundation of Institute of Chemical Materials, China Academy of Engineering Physics (KJCX-201311).

Notes and references

^aInstitute of Chemical Materials and Advanced Materials Research Center, Key Laboratory of Science and Technology on High Energy Laser, China Academy of Engineering Physics, Mianyang, 621900, P. R. China. E-mail: zough@caep.cn; caihuaqiang@caep.cn.

^bFujian Institute of Research on the Structure of Matter, Key Laboratory of Optoelectronic Materials Chemistry and Physics, Chinese Academy of Sciences, Fuzhou, 350002, P. R. China. E-mail: nye@fjirsm.ac.cn

† Electronic Supplementary Information (ESI) available: CSD - 428146. For ESI and crystallographic data in CIF or other electronic format see DOI: 10.1039/b000000x/

- (1) (a) D. A. Keszler, A. Akella, K. I. Schaffers, T. Alekel, *Mater. Res. Soc. Symp. Proc.* 1994, **329**, 15; (b) H. W. Huang, J. Y. Yao, Z. S. Lin, X. Y. Wang, R. He, W. J. Yao, N. X. Zhai, C. T. Chen, *Angew. Chem.* 2011, **123**, 9307; *Angew. Chem. Int. Ed.* 2011, **50**, 9141; (c) S.C. Wang, N. Ye, W. Li, D. Zhao, *J. Am. Chem. Soc.* 2010, **132**, 8779; (d) H. P. Wu, S. L. Pan, K. R. Poeppelmeier, J. M. Rondinelli, *J. Am. Chem. Soc.* 2013, **135**, 4215; (e) C. D. McMillen, J. T. Stritzinger, J. W. Kolis, *Inorg. Chem.* 2012, **51**, 3953; (f) S. F. Jin, G. M. Cai, W. Y. Wang, M. He, S. C. Wang, X. L. Chen, *Angew. Chem.* 2010, **122**, 5087; *Angew. Chem. Int. Ed.* 2010, **49**, 4967; (g) H. Y. Chang, S. H. Kim, P. S. Halasyamani, K. M. Ok, *J. Am. Chem. Soc.* 2009, **131**, 2426; (h) H. P. Wu, S. L. Pan, K. R. Poeppelmeier, H. Y. Li, D. Z. Jia, Z. H. Chen, X. Y. Fan, Y. Yang, J. M. Rondinelli, H. S. Luo, *J. Am. Chem. Soc.* 2011, **133**, 7786; (i) S. C. Wang, N. Ye, *J. Am. Chem. Soc.* 2011, **133**, 11458; (j) G. H. Zou, N. Ye, L. Huang, X. S. Lin, *J. Am. Chem. Soc.* 2011, **133**, 20001; (k) L. Sun, Y. F. Ling, P. P. Zhang, J. Luo, *Chinese Journal of Energetic Materials*, 2014, **22**, 447; (l) H. Y. Li, S. L. Pan, K. R. Poeppelmeier, *Eur. J. Inorg. Chem.* 2013, **18**, 3185; (m) National Photonics Initiative, "Lighting the Path to a Competitive, Secure Future," May 23, 2013; (n) National Research Council, *Optics and Photonics: Essential Technologies for Our Nation*. Washington, DC: The National Academies Press, 2013; (o) A. H. Reshak, S. Auluck, I. V. Kityk, *J. Phys.: Condens. Matter*, 2008, **20** 145209; (p) A. H. Reshak, S. Auluck, I. V. Kityk, *J. Phys. Chem. A*, 2009, **113**, 1614; (q) A. H. Reshak, D. Stys, S. Auluck, I. V. Kityk, *J. Phys. Chem. B*, 2010, **114**, 1815; (r) A. H. Reshak, S. Auluck, I. V. Kityk, *PHYSICAL REVIEW B*, 2007, **75**, 245120.
- (2) (a) P. S. Halasyamani, K. R. Poeppelmeier, *Chem. Mater.* 1998, **10**, 2753; (b) H. Ye, D. Fu, Y. Zhang, W. Zhang, R. G. Xiong, S. D. Huang, *J. Am. Chem. Soc.* 2009, **131**, 42; (c) A. H. Reshak, X. Chen, I. V. Kityk, S. Auluck, K. Iliopoulos, S. Couris, R. Khenata, *Current Opinion in Solid State and Materials Science*, 2008, **12**, 26; (d) A. H. Reshak, X. Chen, S. Auluck, I. V. Kityk, *THE JOURNAL OF CHEMICAL PHYSICS*, 2008, **129**, 204111; (e) A. H. Reshak, X. Chen, F. P. Song, I. V. Kityk, S. Auluck, *J. Phys.: Condens. Matter*, 2009, **21**, 205402; (f) A. H. Reshak, S. Auluck, I. V. Kityk, *J. Phys. D: Appl. Phys.* 2009, **42**, 085406.
- (3) (a) H. S. K. Ra, K. M. Ok, P. S. Halasyamani, *J. Am. Chem. Soc.* 2003, **125**, 7764; (b) R. E. Sykora, K. M. Ok, P. S. Halasyamani, T. E. Albrecht-Schmitt, *J. Am. Chem. Soc.* 2002, **124**, 1951; (c) E. O. Chi, K. M. Ok, Y. Porter, P. S. Halasyamani, *Chem. Mater.* 2006, **18**, 2070.
- (4) (a) W. L. Zhang, W. D. Cheng, H. Zhang, L. Geng, C. S. Lin, Z. Z. He, *J. Am. Chem. Soc.* 2010, **132**, 1508; (b) Y. Inaguma, M. Yoshida, T. Katsumata, *J. Am. Chem. Soc.* 2008, **130**, 6704.
- (5) D. Phanon, I. Gautier-Luneau, *Angew. Chem., Int. Ed.* 2007, **46**, 8488.
- (6) P. Becker, *Adv. Mater.* 1998, **10**, 979.
- (7) Y. Z. Huang, L. M. Wu, X. T. Wu, L. H. Li, L. Chen, Y. F. Zhang, *J. Am. Chem. Soc.* 2010, **132**, 12788.
- (8) C. F. Sun, C. L. Hu, X. Xu, J. B. Ling, T. Hu, F. Kong, X. F. Long, J. G. Mao, *J. Am. Chem. Soc.* 2009, **131**, 9486.
- (9) (a) C. T. Chen, B. C. Wu, A. D. Jiang, G. M. You, *Sci. Sin. B-Chem. Biol. Agr. Med. Earth Sci.* 1985, **28**, 235; (b) Y. C. Wu, T. Sasaki, S. Nakai, A. Yokotani, H. G. Tang, C. T. Chen, *Appl. Phys. Lett.* 1993, **62**, 2614; (c) Y. Mori, I. Kuroda, S. Nakajima, T. Sasaki, S. Nakai, *Appl. Phys. Lett.* 1995, **67**, 1818; (d) J. M. Tu, D. A. Keszler, *Mater. Res. Bull.* 1995, **30**, 209; (e) C. T. Chen, Y. B. Wang, B. C. Wu, K. C. Wu, W. L. Zeng, L. H. Yu, *Nature* 1995, **373**, 322; (f) H. W. Yu, S. L. Pan, H. P. Wu, Z. H. Yang, *J. Mater. Chem.* 2012, **22**, 2105; (g) G. H. Zou, Z. J. Ma, K. C. Wu, N. Ye, *J. Mater. Chem.* 2012, **22**, 19911.
- (10) (a) A. D. Mills, *Inorg. Chem.* 1962, **1**, 960. (b) A. A. Ballman, *Am. Mineral.* 1962, **47**, 1380. (c) E. L. Belokoneva, A. V. Azizov, N. I. Leonyuk, M. A. Simonov, *J. Struct. Chem.* 1981, **22**, 476.
- (11) N. Ye, J. L. Stone-Sundberg, M. A. Hruschka, G. Aka, W. Kong, D. A. Keszler, *Chem. Mater.* 2005, **17**, 2687.
- (12) (a) G. Aka, A. Kahn-Harari, D. Vivien, J.M. Benitez, F. Salin, J. Godard, *Eur. J. Solid State Inorg. Chem.* 1996, **33**, 727; (b) M. Iwai, T. Kobayashi, H. Furuya, Y. Mori, T. Sasaki, *Jpn. J. Appl. Phys.* 1997, **36**, 276.
- (13) (a) M. D. Segall, P. J. D. Lindan, M. J. Probert, C. J. Pickard, P. J. Hasnip, S. J. Clark, M. C. Payne, *J. Phys.: Condens. Matter*, 2002, **14**, 2717; (b) V. Milman, B. Winkler, J. A. White, C. J. Pickard, M. C. Payne, E. V. Akhmatkaya, R. H. Nobes, *Int. J. Quantum Chem.*, 2000, **77**, 895.
- (14) J. P. Perdew, K. Burke, M. Ernzerhof, *Phys. Rev. Lett.*, 1996, **77**, 3865.
- (15) J. R. Hughes. Thomas, R. Feijoo. Gonzalo, Mazzei. Luca, *Computer Methods in Applied Mechanics and Engineering*, 1998, **166**, 3.
- (16) J. S. Lin, A. Qteish, M. C. Payne, V. Heine, *Phys. Rev. B*, 1993, **47**, 4174.
- (17) (a) I. D. Brown, D. Altermatt, *Acta Crystallogr.* 1985, **B41**, 244; (b) N. E. Brese, M. O'Keeffe, *Acta Crystallogr.* 1991, **B47**, 192.
- (18) (a) J. H. Lin, L. P. You, G. X. Lu, L. Q. Yang, M. Z. Su, *J. Mater. Chem.*, 1998, **8**, 1051; (b) W. W. Zhao, S. L. Pan, J. Han, Z. X. Zhou, X. L. Tian, J. J. Li, *Inorg. Chem. Commun.*, 2011, **14**, 566.
- (19) S. K. Kurtz, T. T. Perry, *J. Appl. Phys.* 1968, **39**, 3798.
- (20) (a) P. Kubelka, F. Z. Munk, *Tech. Phys.*, 1931, **12**, 593; (b) J. Tauc, *Mater. Res. Bull.* 1970, **5**, 721.
- (21) G. M. Sheldrick, *Acta Crystallogr. Sect. A*, 2008, **64**, 112.
- (22) A. L. Spek, *J. Appl. Crystallogr.* 2003, **36**, 744.
- (23) R. C. Eckardt, H. Masuda, Y. X. Fan, R. L. Byer, *IEEE J. Quantum Electron. QE*, 1990, **26**, 922.